Multiscale Observation of Multiple Moving Targets using Micro Aerial Vehicles

Asif Khan[1,2], Bernhard Rinner[1], Andrea Cavallaro[2]

***Abstract*— This paper presents a centralized algorithm for multi-scale observation of multiple moving targets using a team of Micro Aerial Vehicles (MAVs). The proposed algorithm is appropriate when MAVs can observe targets at different elevations with the objective of jointly maximizing duration and resolution of observation for each target. The MAVs share the workload using a greedy assignment of locations and targets to MAVs. The proposed algorithm uses a quad-tree data structure to model the movement decisions of MAVs as well as the variable qualities (resolutions) of observations. We consider cases where there is uncertainty in the target observations (i.e., measurement noise), the number of targets is larger than that of the MAVs and the combined field of views (FOVs) of the sensors cannot cover the whole search region. Simulation results confirm the effectiveness of the proposed algorithm.**

I. INTRODUCTION

Many search and rescue, reconnaissance and surveillance tasks require a team of cooperating robots that monitor multiple moving targets [1], [2], [3]. Other applications of such cooperative observation of multiple moving targets can be found in sports [4], crowd and social movement monitoring [5] and wildlife research [6]. Existing works have mostly focused on ground robots [7] and consider *perfect* sensors [7] that are not affected by noise or detection errors (i.e., false and miss detection).

The versatility of Micro Aerial Vehicles (MAVs), such as quad-rotors [8], favours their use as multi-MAV systems to observe a scene from different viewpoints [9], [10] and at different spatial scales (resolutions) [11], [12], [2], [3], [6], [8]. A key research problem is the dynamic placement of these MAVs to maximize the observation of the number targets as well as the resolution (i.e., quality) of observation.

The use of a cooperative team of autonomous sensor-based homogeneous robots for observing multiple moving targets, also known as Cooperative Multi-robot Observation of Multiple Moving Targets (CMOMMT), is an NP-hard problem [1]. CMOMMT considers a greater number of targets than robots and develops a dynamic placement strategy for ground robots to maximize the collective time during which each target is observed. Each robot operates either in *search* or *track* mode. When a robot finds one or more targets in its FOV, it tracks them and moves toward the virtual center of mass of the moving targets. A robot is attracted to the near-by targets to keep close enough to observe them and repulsed by neighbor robots to avoid observation overlap. The robot switches back to search mode when there are no targets in its FOV.

CMOMMT using local force vectors [1] for coordination among robots was upgraded to Approximate CMOMMT (A-CMOMMT) by including weighted local force vectors [13], [14] and P-CMOMMT [15] by reducing the overlap of observation of a single target by multiple robots. To reduce the risk of losing a target, Behavioral CMOMMT (B-CMOMMT) [16], [7] adds a third mode of operation, namely the *help* mode: a robot that it is about to lose a target broadcasts a help request to other robots. The robots in search mode respond to this request by approaching the robot that issued the request. A similar approach was also proposed in [17] by assigning different priority weights to targets. Instead of using local force vectors and help calls, flexible formation of robots [18] and model-predictive control strategies [19] can be used in CMOMMT. Important parameters are the degree of decentralization [20] and the minimization of the time of initial contact with a newly generated target [21].

More recent methods use MAVs to increase the observation of moving targets [22], [23]. Existing CMOMMT approaches [1], [13], [14], [15], [7], [19], [21] and MAV-based observation of moving targets are based on uniform FOV and uniform resolution observations. A tool for multiscale observation using MAV is quad-tree [11], [12], which was explored only for searching *stationary* targets with a *single* MAV. Works on multiscale observation using a multi-MAV system [10] are limited to the coverage of *static* environments without any targets. Moreover, sensing limitations such as measurement noise, miss-detections and false positives are ignored in most approaches. Finally, cooperation among robots is based primarily on attractive and repulsive forces without planning.

In this paper, we extend the conventional CMOMMT fixed-altitude or fixed-FOV-size problem to multiscale observations using a multi-MAV system with noisy sensors. We modify the CMOMMT objective function by including a term that accounts for the resolution of observation. To model observations at large spatial scales (low resolution) versus observations at a small spatial scales (high resolution), we use a quad-tree to help in defining the tradeoff between the visibility and the quality of observations of multiple moving targets. Unlike conventional CMOMMT approaches, we also model sensing errors in the form of measurement noise when reporting the location of a target.

Asif Khan was supported by the EACEA Agency of the European Commission under EMJD ICE (FPA no 2010- 0012). The work has also been supported by the ERDF, KWF, and BABEG under grant KWF-20214/24272/36084 (SINUS) and has been performed in the research cluster Lakeside Labs GmbH.

[1]Institute of Networked and Embedded Systems, Alpen-Adria-Universität Klagenfurt, Lakeside Labs GmbH, Klagenfurt 9020 Austria.

[2]Centre for Intelligent Sensing, Queen Mary University of London, London E1 4NS, UK

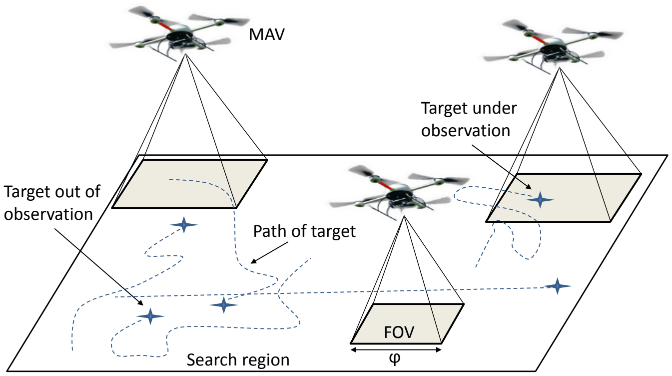

Fig. 1: Observing multiple moving targets using cooperative MAVs.

The rest of this paper is organized as follows. In Section II, we formulate the problem. Section III defines the objective function. Section IV discusses the proposed approach for multi-scale observation of moving targets. In Section V, we discuss simulation results. Finally, in Section VI we conclude the paper and discuss future work.

II. Problem Formulation

Let us consider an obstacle free, rectangular and bounded search region $\Omega \in \mathbb{R}^2$ with known dimensions (length l and width w). Let $\mathbf{G} = \{G_1, G_2, ..., G_B\}$ be a set of B moving, non-cooperative, non-evasive and uniquely identifiable targets in Ω. The value of B is assumed to be known and constant during the mission. The state of the j^{th} target at time t is denoted by

$$\mathbf{x}_j^t = (x_j^t, \dot{x}_j^t, y_j^t, \dot{y}_j^t), \tag{1}$$

where (x_j^t, y_j^t) and $(\dot{x}_j^t, \dot{y}_j^t)$ are the position and velocity of the target. The motion of G_j is

$$\mathbf{x}_j^{t+1} = \Phi \mathbf{x}_j^t + \gamma_j, \tag{2}$$

where Φ is the state transition matrix with process noise $\gamma_j \backsim \mathcal{N}(0, Q)$ and process noise covariance matrix Q. The movement of the targets is independent of each other and the location of the targets in Ω is initially unknown.

Let $\mathbf{U} = \{U_1, U_2, ..., U_A\}$ be a set of A homogeneous and synchronized MAVs moving above the search region Ω in discrete time t (Fig. 1). The value of A is known. The state of the i^{th} MAV at time t is

$$\mathbf{y}_i^t = (x_i^t, y_i^t, z_i^t), \tag{3}$$

which defines the position of the MAV U_i in space. The MAVs are assumed to move above the region Ω and thus the (x, y) components of $\mathbf{y}_i^t$ coincide with $(x, y) \in \Omega$. Because of spatial quantization, we assume that more than one MAVs can go to the same location and have the same state.

At time step t, each MAV executes the following three actions: takes observation, receives new location for movement, and moves to the new location. We assume that $A \ll B$ and that the speed of each MAV is higher than that of the fastest target. The MAV can hover at a specific location and there is no constraint on its turning angle.

We assume that each MAV is equipped with a position sensor (e.g., GPS) a surveillance sensor to observe Ω, a wireless communication unit to exchange information with a ground station, and a computing unit to perform updates and local control actions.

The surveillance sensor of the MAV U_i consists of a downward-looking camera with a constant zoom level. The MAV U_i varies its FOV F_i by changing its altitude[1] z_i. For simplicity we consider the FOV $F_i \in \Omega$ of MAV U_i to be a square with side of length φ (Fig. 1).

A target is considered under observation when it is in the FOV of at least one MAV. The observation of target G_j by MAV U_i at time t is defined as

$$O_{ij}^t = \begin{cases} 1 & \text{if } (x_j^t, y_j^t) \in F_i \\ 0 & otherwise. \end{cases} \tag{4}$$

A single MAV can observe multiple targets and a single target can be observed by multiple MAVs. However, the observation of a single target by multiple MAVs at time t is of no advantage as we are not interested in depth perception, multi-view analysis or in obtaining a good estimate of the target position. We use the OR operator [1] to show that observation by a single MAV is sufficient:

$$\bigvee_{i=1}^{A} O_{ij}^t = \begin{cases} 1 & \text{if } \exists i : O_{ij}^t = 1 \\ 0 & otherwise. \end{cases} \tag{5}$$

The MAV U_i collects a measurement $\mathbf{z}_{ij}^t$ for target G_j under its observation. The measurement $\mathbf{z}_{ij^t}$ consists of the observed target state for G_j. At time t, there can be $n_i^t \leq B$ targets in F_i and thus n_i^t measurements can be generated. A measurement $\mathbf{z}_{ij}^t$ taken by the MAV U_i for target G_j at time t is generated by the following model

$$\mathbf{z}_{ij}^t = \mathbf{H}\mathbf{x}_j^t + \vartheta, \tag{6}$$

where $\mathbf{H} = (1\ 0\ 0\ 0; 0\ 0\ 1\ 0)$ is the observation matrix with observation noise $\vartheta \backsim \mathcal{N}(0, R)$ and observation noise covariance matrix R. Sensing errors (Eq. 6) can misguide the MAV movement, which in turn may cause a target to escape from observation. The states of all the targets, all the MAVs, and the measurements for all the targets are denoted as $\mathbf{X}^t = \{\mathbf{x}_1^t, \ldots, \mathbf{x}_B^t\}$, $\mathbf{Y}^t = \{\mathbf{y}_1^t, \ldots, \mathbf{y}_A^t\}$ and $\mathbf{Z}^t = \{\mathbf{z}_1^t, \ldots, \mathbf{z}_B^t\}$, respectively.

III. Multi-resolution objective function

The standard CMOMMT [13], [14], [15], [7], [17] problem maximizes the collective time of observation represented by the following objective function

$$\Upsilon = \sum_{t=0}^{\Gamma} \sum_{j=1}^{B} \bigvee_{i=1}^{A} O_{ij}^t, \tag{7}$$

[1]The method is equally applicable to constant-altitude MAVs with variable zoom levels (z_i).

where Γ is the total time of the mission. We extend the CMOMMT problem formulation to include variable resolution of observations and measurement noise. We refer to this problem as *multi-scale observation of multiple moving targets*.

A higher value of the altitude z increases the FOV but reduces the resolution of observation (i.e., the spatial scale the target is being observed at). The variable resolution observations can also improve the movement decisions of the MAVs in order to maximize the number of targets under observation. Reducing the value of z from the surface of search region improves the resolution of observation. However, we set a minimum allowed altitude z_0, as reducing altitude of the MAV below z_0 may cause the MAV to hit the target.

The resolution of observation of target G_j by MAV U_i at time t is defined as

$$r_{ij}^t = \begin{cases} \frac{1}{z_i^t} & \text{if } (x_j^t, y_j^t) \in F_i^t \\ 0 & otherwise. \end{cases} \quad (8)$$

In case of multiple MAVs observing a target G_j with different resolutions, the resolution used is given as

$$\hat{r}_j^t = max\{r_{1j}^t, ..., r_{Aj}^t\}. \quad (9)$$

In addition to maximizing the collective time of observation, we want to maximize the collective resolution of observations.

Maximizing the collective resolution of observation of the targets under observation corresponds to maximizing the following objective function:

$$\Psi = \sum_{t=0}^{\Gamma} \sum_{j=1}^{B} \hat{r}_j^t. \quad (10)$$

With limited number of MAVs (i.e., $A < B$) not all targets might be under observation and it is not possible to observe all the targets with high resolution all the time. The goal thus becomes to maximize

$$g = \frac{1}{b\Gamma} \Bigg(\alpha \Upsilon + (1 - \alpha) \Psi \Bigg), \quad (11)$$

where $g \in [0, 1]$, $g = 0$ implies that no target is under observation throughout the mission and $g = 1$ implies that all the targets are under observation with the desired resolution throughout the mission. The parameter α assigns a priority weight or importance to the resolution of observation. Setting $\alpha = 1$ makes the problem as a standard CMOMMT problem with constant FOV and no interest in high resolution observations.

In Table I, we provide some numeric values of g for B targets and mission duration of Γ time steps. These values are calculated by putting Υ (Eq. 7) and Ψ (Eq. 10) in Eq. 11 for two different values of Γ and α. Setting $\alpha = 0$ means that we want to maximize the collective resolution of observations of the targets that are currently under observation. Note that it is difficult to get $g = 1$ for $\alpha = 0$, as targets will easily escape the smallest FOV. The multi-scale multi-MAV coverage problem at hand is dynamic and, at each time step, the coordinated movement approach should determine which MAVs observe, the part of the search region to observe, and the resolution of observation. We focus on developing a centralized cooperation and movement strategy for a team of MAVs to maximize g.

TABLE I: Duration of observation and resolution of observation for B targets, mission duration of Γ time steps, and highest resolution $1/z_0$ (z_0 is lowest altitude).

	$\Gamma/2$	Γ
Lowest resolution ($\alpha = 1$)	$g = 0.5$	$g = 1$
Highest resolution ($\alpha = 0$)	$g = 1/z_0$	$g = 1/2z_0$

IV. QUAD-TREE BASED SPACE DISCRETIZATION

We discretize and model the 3D space for the movement of MAVs as a quad-tree τ [24] with κ nodes. Let d denote the depth of the tree where the root node is at $d = 1$ and the leaf nodes are at maximum depth of $d = \varepsilon$. In the proposed framework, the topology of the tree is fixed (nodes cannot be added or deleted) and complete (all its leaves are at the same depth). Except the root and the leaf nodes, each node k has five adjacent nodes, i.e., k_0 (parent node) and four children nodes k_1 (north west), k_2 (north east), k_3 (south east), k_4 (south west). The levels of the quad-tree are related to the minimum allowable altitude as

$$z = 2^{\varepsilon - d} z_0. \quad (12)$$

By considering the value of z in Eq. 8 and dividing by z_0 yields the normalized value $r_i \leq 1$ for the resolution of observation made by MAV U_i at depth d_i

$$r_i = \frac{1}{2^{\varepsilon - d_i}}. \quad (13)$$

Each node represents an allowable location for the movement of MAVs, such that $\mathbf{y}_i^t = k$ for $k = \{1, 2, ..., \kappa\}$. Every node is associated with a FOV. Any MAV U_i that hovers at node k will always have a specific FOV, denoted as $F_i = F_k \subset \Omega$. If k is an internal node and $k_1, ..., k_4$ are its children, then the various F_{k_i} are obtained by splitting the F_k into four equally sized squares. Therefore $F_k = \cup_{i=1,2,3,4} F_{k_i}$ and $F_{k_i} \cap F_{k_j} = \emptyset$ where k_i and k_j are siblings. It is obvious that a MAV at node k with FOV F_k is already observing $F_{k_1}, F_{k_2}, F_{k_3}, F_{k_4}$ with resolution r_k. An MAV can only take observation when located at a node of τ as shown in Fig. 2a.

The root of the quad-tree τ is centered at Ω, such that $F_\tau = \Omega$ and leaf nodes are at $z = z_0$. This centralized quad-tree is used as a coordination mechanism among MAVs. The key purpose of the quad-tree is to reduce the movement options from 27 in an unconstrained neighborhood cube to only 14 (including the current position). These fourteen nodes include the current node k, 8 nearest nodes on the same level of the quad-tree $\hat{k}_1, ...\hat{k}_8$, the parent node k_0, and 4 children nodes $k_1, ..., k_4$. The exceptions are the root node (5 movement options), the leaf node (10 movement options), and nodes on $d = 2$ (9 movement options). The

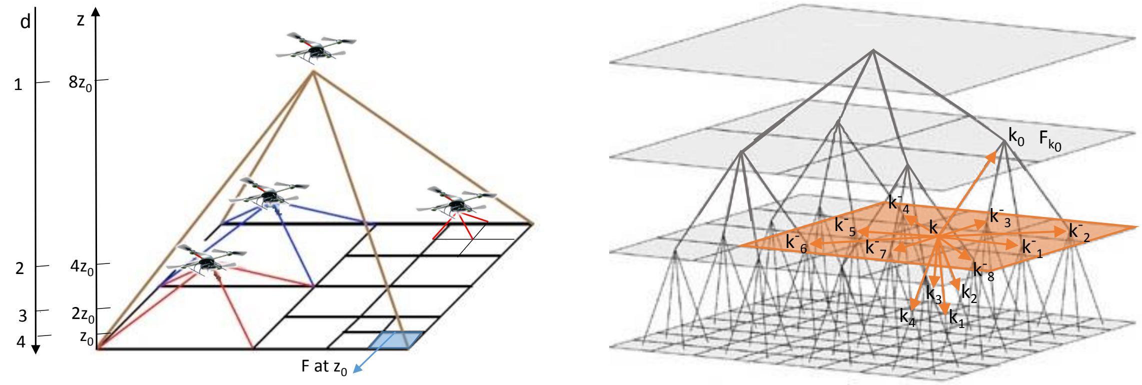

(a) (b)

Fig. 2: Model for the MAV movement: (a) Relationship of search region Ω, FOV (F), altitude (z), lowest altitude (z_0), and depth (d) of the quad-tree. (b) Fourteen-neighborhood (orange arrows and square around the current node k).

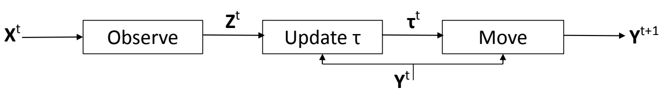

Fig. 3: Block diagram of the overall process in a single time step.

fourteen movement options for a MAV hovering at node k are shown in Fig. 2b. We do not need 27 movement locations, because increasing the altitude reduces the number of movement locations as $\bigcup_{e\in E} F_e = \Omega$, where E is the set of nodes at any given depth d.

Fig. 3 shows the overall process in a single time step. The MAVs observe the targets' actual states $\mathbf{X}^t$ at time step t and generate the measurements $\mathbf{Z}^t$. Information about the target locations $\mathbf{Z}^t$ and current states of all the MAVs $\mathbf{Y}^t$ at time step t are used to update the centralized quad-tree τ. This updated quad-tree and the current states of all the MAVs are then used to move each MAV to one of 14 neighboring locations.

The objective of MAV movement decision is to appropriately identify the nodes of the τ that maximize the number of targets under observation and their resolution. These nodes are identified and assigned to the MAVs as waypoints at each time step.

The ground station maintains the centralized quad-tree τ. In addition to $\mathbf{y}_i$, each node of the quad-tree τ maintains the following value

$$v_k = \frac{\alpha n_k + (1-\alpha) n_k r_k}{1 + m_k}, \tag{14}$$

where n_k is the number of targets visible under node k, m_k is the number of MAVs hovering at node k and r_k is the resolution of observation taken by a MAV hovering at node k (Eq. 13). An increase in the depth of node k or the number of targets visible from node k increases the value of v_k. The term m_k in the denominator introduces the spread among the MAVs. In our proposed algorithm, the ground station identifies and assigns nodes to the MAVs that maximizes the team's dispersion pattern, number of targets under observation, and resolution of observation. The movement decision takes into account two sub-goals, namely maximization of the number of targets under observation and resolution maximization. While the MAVs can be trapped in a local maximum, the effects of this local maximum are likely to be temporary as targets move.

The value of v_k cannot be determined accurately when F_k contains one or more targets and F_k is not observed by any MAVs. The states of such unobserved targets are estimated using Eq. 2 and last known locations of these unobserved targets. To include uncertainty in these estimated target states we use process noise covariance matrix $\overline{Q}$ which is greater in magnitude than Q. We assume a random location in the unobserved part of Ω as an estimate of the target for which no information is available.

The centralized controller determines the new positions for all the MAVs, as presented in Algorithm 1. At each time step, the new positions are determined sequentially starting from U_1 to U_A (line 15 in Algorithm 1). To find the new position for a MAV U_i two steps are required. First, states for the unobserved targets, if any, are estimated (line 16 to line 20) and measurements $\mathbf{z}_j$ (Eq. 6) about the target locations are made. These measurements are used to calculate the value of n_k. Second, the value v_k for all the nodes in τ is updated (line 21 to 23). The values of n_k and r_k required to update v_k are determined from MAV observations (Eq. 6) and estimated states of unobserved targets (line 16 to line 20). The value of m_k is updated in each iteration of the outer loop (line 15). Third, the new position $\mathbf{y}_i^{t+1}$ for MAV U_i is determined (line 27). This new position is one of fourteen adjacent positions (including the current node) that has the maximum value of v_k. If more than one node has the same value of v_k, priority is given to the node at higher depth level (to reduce the altitude of the MAV). If more than one node on one level of the quad-tree has same value of v_k, priority is given to the node that comes first in the anti-clockwise direction. These priorities are taken into account in line 25 and line 26 of Algorithm 1 by sorting the 14 nodes around node k into a temporary

Algorithm 1 MAVs movement.

1: A: number of MAVs
2: B: number of targets
3: $\mathbf{x}_j^t$: state of target G_j at time step t
4: $\mathbf{y}_i^t$: state of MAV U_i at time step t
5: Φ: transition matrix (Eq. 2)
6: γ_j: $\mathcal{N}(0, \overline{Q})$ process noise (Eq. 2)
7: m_k: number of MAVs at node k
8: n_k: number of targets visible from node k
9: r_k: resolution associated with node k (Eq. 13)
10: $temp$: temporary array to store 14 nodes priority-wise
11: s: temporary variable to store the current state U_i
12: Initialize quad-tree τ by setting $v_k = 0$ for $k = 1, ..., \kappa$
13: Initialize the MAV states $\mathbf{Y}^0$
14: **procedure** MOVEMAVS($\tau, \mathbf{Y}^t$)
15:     **for** $i = 1 : A$ **do**
16:         **for** $j = 1 : B$ **do**
17:             **if** $O_j == 0$ **then**
18:                 $\mathbf{x}_j^t = \Phi \mathbf{x}_j^{t-1} + \gamma_j^{t-1}$
19:             **end if**
20:         **end for**
21:         **for** $k = 1 : \kappa$ **do**
22:             $v_k = \frac{\alpha n_k + (1-\alpha) n_k r_k}{1 + m_k}$
23:         **end for**
24:         $s \leftarrow \mathbf{y}_i^t$
25:         $temp \leftarrow [s_1,\ s_2,\ s_3,\ s_4,\ s,\ s_1^-\ s_2^-\ s_3^-\ s_4^-\ s_5^-$
26:             $s_6^-\ s_7^-\ s_8^-,\ s_0]$
27:         $\mathbf{y}_i^{t+1} \leftarrow$Node in $temp$ with maximum value of v
28:     **end for**
29:     **Output** $\mathbf{Y}^{t+1}$
30: **end procedure**

array $temp$. The node in $temp$ with a maximum value of v is determined as the new position for MAV U_i (line 27). After loop termination (line 29), the ground station has new positions $\mathbf{Y}^{t+1}$ for all the MAVs. These new positions/states are sent to MAVs for taking further observations.

V. Simulation results

We perform simulations for a region Ω of $l \times w = 4096 \times 4096\ m^2$, mission duration of $\Gamma = 1000$ time steps, $Q = 0.1 \times I_{4\times4}$, $\overline{Q} = 1 \times I_{4\times4}$, target velocity of $v = 5\ m/s$, and a quad-tree τ of five levels ($\varepsilon = 5$). Knowing the dimensions of the Ω, and ε the τ is initialized with $v_k = 0, k = 1, 2, ..., \kappa$. We initialize the location of each MAV from the root of the quad-tree, unless otherwise stated. Fig. 4 shows the search region with paths of $B = 8$ targets, initialized at random locations and random directions.

We show the observations and their associated depths of the quad-tree (d) for eight targets ($B = 8$) and a team of three MAVs ($A = 3$) in Fig. 5a and Fig. 5b. The results are the average of 100 runs of simulations for different target tracks. Higher values of α affect the movement of MAVs to increase the number of targets under observation but do not care for quality of observation. Reducing the value of α affects the movement of MAVs by forcing them towards leaf

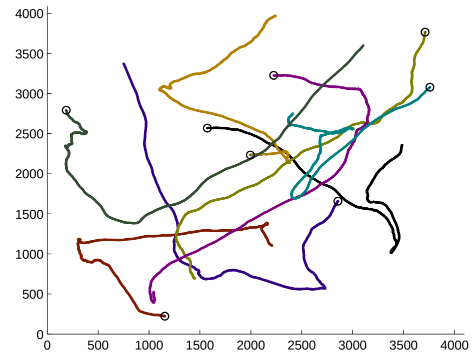

Fig. 4: Paths of $B = 8$ targets for $\Gamma = 1000$ time steps. Black circles show the starting points of the paths.

nodes $d = 5$. Fig. 5b shows that, on average, all the targets are observed at high resolution.

The time evolution of paths for $A = 3$ MAVs observing $B = 8$ targets is shown in Fig. 6. The MAVs U_1 and U_3 start observing targets with highest resolution during the first $\Gamma = 100$ time steps. The MAV U_2 cannot reduce the altitude because it would make more targets unobserved. Throughout the mission, the MAVs vary their altitudes to avoid empty FOV and large number of targets being unobserved.

The effect of changing the number of MAVs and targets

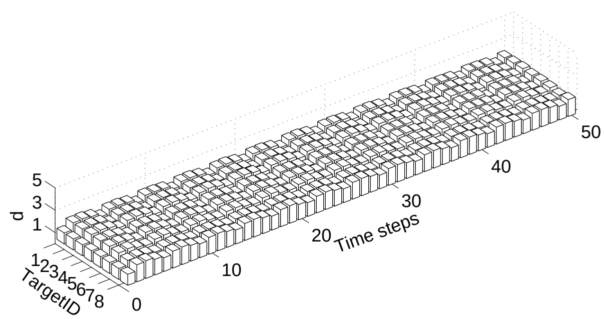

(a) $\alpha = 0.9$.

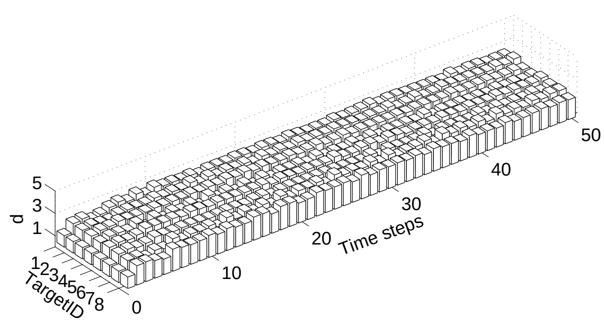

(b) $\alpha = 0.1$.

Fig. 5: Observations and their associated quad-tree depths for $B = 8$ targets and $A = 3$ MAVs.

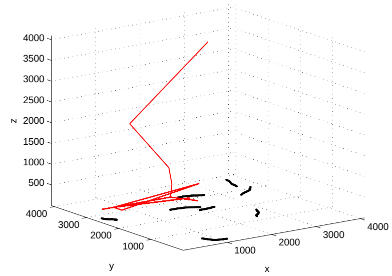

(a) $U_1, \Gamma = 100$.

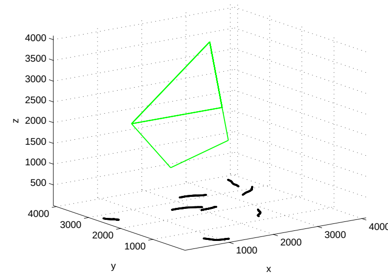

(b) $U_2, \Gamma = 100$.

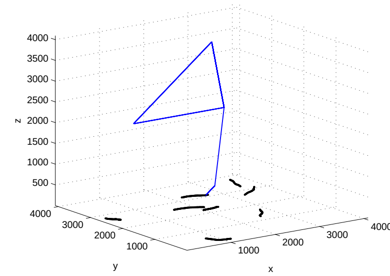

(c) $U_3, \Gamma = 100$.

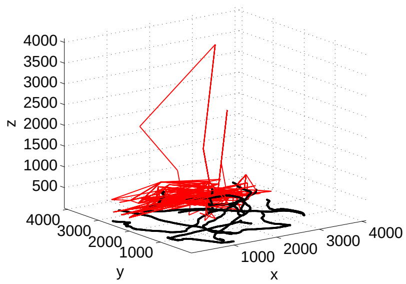

(d) $U_1, \Gamma = 1000$.

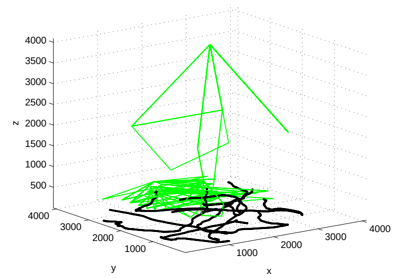

(e) $U_2, \Gamma = 1000$.

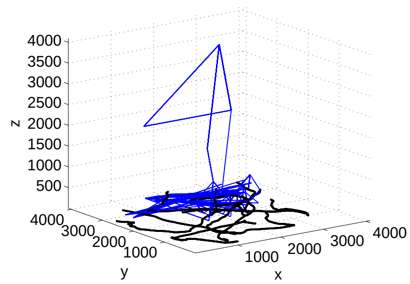

(f) $U_3, \Gamma = 1000$.

Fig. 6: Sample paths of $A = 3$ MAVs ($\alpha = 0.1$).

on the performance measure (Eq. 11) is shown in Fig. 7. The figure shows how the approach scales with the number of targets and MAVs. The increase in the number of MAVs (A) for a given value of B and a given value of α always increases the resolution observation of targets (g). Increasing the number of targets (B) results in the following four different trends, which are caused by different values of A and α: (i) smaller values of both α and A result in slower increase of g; (ii) the combination of smaller value of α and larger value of A decreases g; (iii) the combination of larger value of α and smaller value of A increases g; and (iv) larger values of both α and A decrease g. It is clear from Fig. 7 that the value of g for different values of A converges as we decrease the value of the ratio A/B. This convergence is faster for higher values of α. A decrease of α compels the MAVs to reduce their altitudes getting more targets out of observation, which reduces not only the value of g but also the convergence to same value of performance measure. Therefore, a decrease in α for given values of A and B decreases the value of g.

We show the effect of the quad-tree size on the performance measure (Eq. 11) in Fig. 8. We perform the simulation for the quad-tree ranging in size from one level (only one node, $\varepsilon = 1$) to seven levels ($\varepsilon = 7$, 4096 leaf nodes and 21845 total nodes). It is clear from Fig. 8 that the size of the quad-tree does not affect the performance for $\alpha = 1$. Because the MAVs will always increase altitude to observe the whole region. However, for smaller values of α, increase in size of the quad-tree abruptly increases the performance. We find that allowing more locations for the MAV movement can maximize both the collective time and collective resolution of observation.

The MAV location initialization also affects the performance of our proposed approach. The effect of MAV location initialization is shown in Fig. 9. We perform one simulation by initializing all the MAVs at the root node of τ and one simulation by initializing all MAVs at random leaf nodes. We plot

$$g_t = \frac{1}{B} \sum_{j=1}^{B} \left(\alpha \bigvee_{i=1}^{A} O_{ij}^t + (1-\alpha) \bigsqcup_{i=1}^{A} r_{ij}^t \right) \tag{15}$$

for each time step, t, to show the instantaneous performance of our proposed approach. Fig. 9 shows that initialization at root node is better for immediate performance (notice first 50 time steps in Fig. 9). As time passes, performance due to both types of initializations converges to the same value.

The effect of observation noise (Eq. 6) is shown in terms of covariance matrix, which is $R = u \times I_{4\times4}$. We increase the observation noise by increasing the value of u. Fig. 10a and Fig. 10b show the effects of observation noise on g and cost e, respectively. We are interested only in the cost of moving from one depth of the quad-tree to another. The cost incurred by MVA U_i at time step t is defined as

$$c_i^t = \varepsilon - d_i, \tag{16}$$

and the collective cost is

$$e = \sum_{t=1}^{\Gamma} \sum_{i=1}^{A} c_i^t. \tag{17}$$

The results in Fig. 10a and Fig. 10b are average values of 100 simulation runs. While an increased sensor noise does not affect g, it increases the movement cost by moving the MAVs upwards.

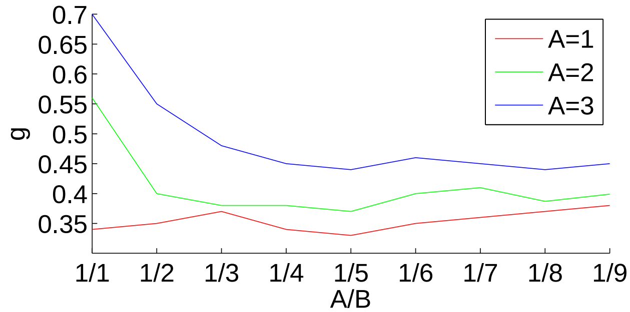

(a) $\alpha = 0.1$

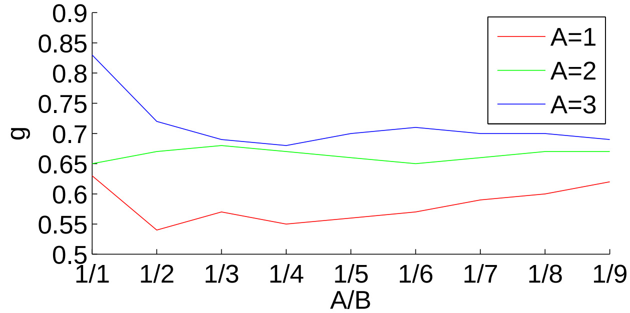

(b) $\alpha = 0.5$

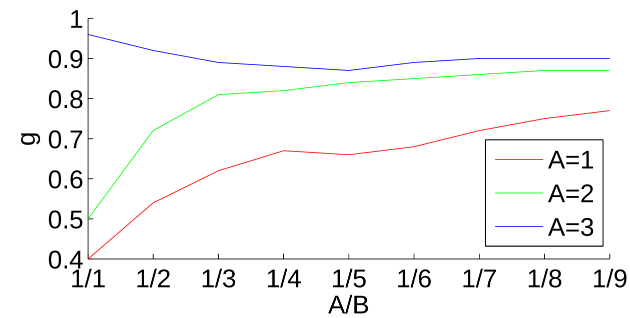

(c) $\alpha = 0.9$

Fig. 7: The effect of the ratio A/B for different values of α.

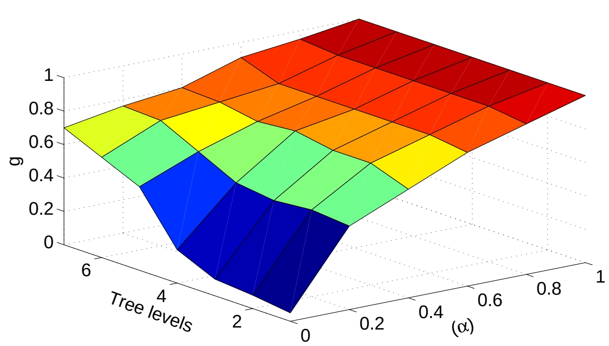

Fig. 8: The effect of the quad-tree size on g ($A = 3, B = 8$).

VI. CONCLUSIONS

We presented a quad-tree based centralized movement strategy for a team of MAVs to maximize the collective time and quality of observation for multiple moving targets.

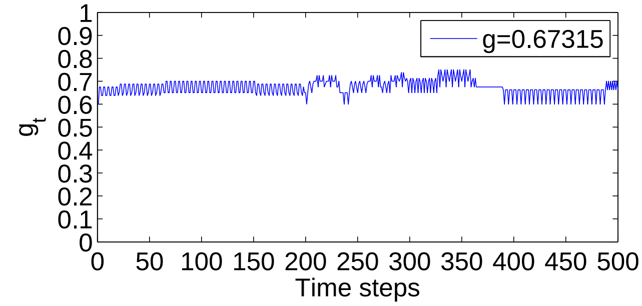

(a) MAVs start at the root node.

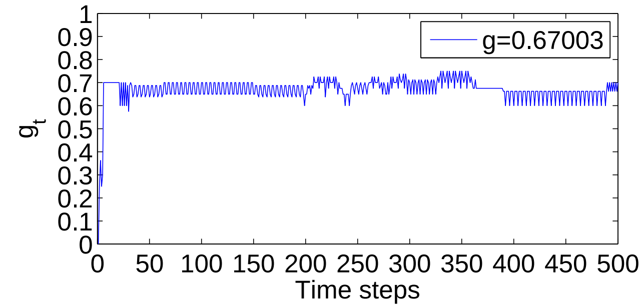

(b) MAVs start at randomly selected leaf nodes.

Fig. 9: The effect of MAV location initialization ($A = 3,\ B = 8,\ \alpha = 0.5$).

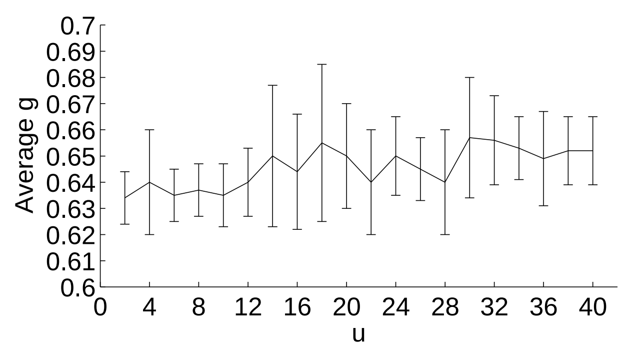

(a)

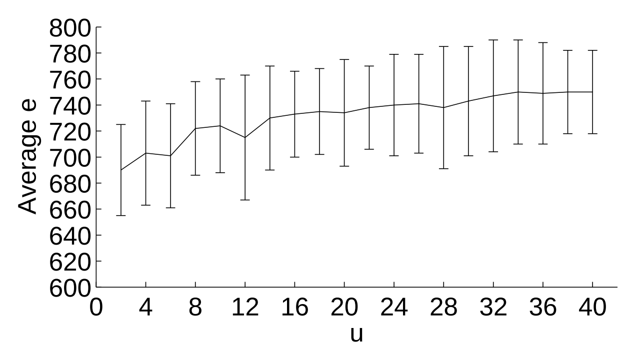

(b)

Fig. 10: The effect of observation noise $R = u \times I_{4\times 4}$ ($A = 3,\ B = 8,\ \alpha = 0.5$).

We also compared two mobility options on the quad-tree for movement of MAVs. This movement strategy enables a team of MAVs to work together towards a common goal of maximizing observation of large group of moving targets. The proposed method is suitable not only for aerial robots that can move in 3D space, but also for sensors that can control the location and zoom level of their FOVs.

Several variations of this dynamic sensor coverage problem are possible, such as considering distributed coordination, heterogeneity of sensors (including pan-tilt-zoom and other parameters of the sensor), the characteristics of the terrain and the cost of movement.

REFERENCES

[1] L. E. Parker and B. A. Emmons, "Cooperative multi-robot observation of multiple moving targets," in *Proc. of the IEEE International Conference on Robotics and Automation*, 1997, pp. 2082–2089.

[2] R. P. Anderson and D. Milutinovic, "A Stochastic Approach to Dubins Vehicle Tracking Problems," *IEEE Transactions on Automatic Control*, vol. 59, no. 10, pp. 2801–2806, 2014.

[3] P. Alberto, C. Pablo, P. Victor, and S. A. Juan, "Ground vehicle detection through aerial images taken by a UAV," in *Proc. of IEEE International Conference on Information Fusion (FUSION)*, 2014, pp. 1–6.

[4] C. Lecher, *How will drones change sports*, 2014. [Online]. Available: http://www.popsci.com/article/technology/how-will-drones-change-sports

[5] B. Livingston, *The Role Of UAVs/MAVs In Domestic Surveillance And Control*. [Online]. Available: http://www.rense.com/general47/uav.htm

[6] A. Rodriguez, J. J. Negro1, M. Mulero1, C. Rodriguez, J. Hernandez-Pliego, and J. Bustamante, "The Eye in the Sky: Combined Use of Unmanned Aerial Systems and GPS Data Loggers for Ecological Research and Conservation of Small Birds," *PLoS ONE*, vol. 7, no. 12, pp. 1–6, 2012.

[7] A. Kolling and S. Carpin, "Cooperative observation of multiple moving targets: an algorithm and its formalization," *The International Journal of Robotics Research*, vol. 26, no. 9, pp. 935–953, 2007.

[8] S. Yahyanejad and B. Rinner, "A fast and mobile system for registration of low-altitude visual and thermal aerial images using multiple small-scale uavs," *ISPRS J. Photogramm. Remote Sens.*, pp. 1–14, 2014.

[9] M. Quaritsch, K. Kruggl, D. Wischounig-Strucl, S. Bhattacharya, M. Shah, and B. Rinner, "Networked UAVs as aerial sensor network for disaster management applications," *Elektrotechnik und Informationstechnik, Special Issue on Wireless Sensor Networks*, pp. 56–63, 2010.

[10] M. Schwager, B. J. Julian, M. Angermann, and D. Rus, "Eyes in the Sky: Decentralized Control for the Deployment of Robotic Camera Networks," *Proceedings of the IEEE*, vol. 99, pp. 1541–1561, 2011.

[11] T. H. Chung and S. Carpin, "Multiscale search using probabilistic quadtrees," in *Proc. of IEEE International Conference on Robotics and Automation*, 2011, pp. 2546–2553.

[12] S. Carpin, D. Burch, N. Basilico, T. H. Chung, and M. Kölsch, "Variable Resolution Search with Quadrotors: Theory and Practice," *J. Field Robotics*, vol. 30, no. 5, pp. 685–701, 2013.

[13] L. E. Parker and C. Touzet, "Multi-robot learning in a cooperative observation task," in *In Distributed Autonomous Robotic Systems 4*. Springer, 2000, pp. 391–401.

[14] L. E. Parker, "Distributed Algorithms for Multi-Robot Observation of Multiple Moving Targets," *Autnomous Robots*, vol. 12, pp. 231–255, 2002.

[15] Y. Ding, M. Zhu, Y. He, and J. Jiang, "P-cmommt algorithm for the cooperative multi-robot observation of multiple moving targets," in *Proc. of the 6th World Congress on Intelligent Control and Automation*, 2006, pp. 9267–9271.

[16] A. Kolling and C. Stefano, "Multirobot cooperation for surveillance of multiple moving targets - a new behavioral approach," in *Proc. of the IEEE International Conference on Robotics and Automation*, 2006, pp. 1311–1316.

[17] B. B. Werger and M. J. Mataric, "Broadcast of Local Eligibility for Multi-Target Observation," *Distributed Autonomous Robotic Systems 4*, pp. 347–356, 2000.

[18] Y. Ding and Y. He, "Flexible formation of the multi-robot system and its application on cmommt problem," in *Proc. of the 2nd International Asia Conference on Informatics in Control, Automation and Robotics*, 2010, pp. 377 – 382.

[19] J. Kuhn, C. Reinl, and O. von Stryk, "Predictive control for multi-robot observation of multiple moving targets based on discrete-continuous linear models," in *Proc. of the 18th World Congress, The International Federation of Automatic Control*, 2011, pp. 257 – 262.

[20] S. Luke, K. Sullivan, L. Panait, and G. Balan, "Tunably decentralized algorithms for cooperative target observation." in *Technical report, Department of Computer Science, George Mason University*, 2004, pp. 1311–1316.

[21] R. A. Coogle and A. M. Howard, "The iceberg observation problem: Using multiple agents to monitor and observe ablating target sources," in *Proc. of the IEEE International Conference on Systems, Man, and Cybernetics*, 2013, pp. 1660–1665.

[22] E. W. Frew and J. Elston, "Target assignment for integrated search and tracking by active robot networks," in *Proc. of IEEE International Conference on Robotics and Automation*, 2008, pp. 2354–2359.

[23] J. P. How, C. Fraser, K. C. Kulling, L. F. Bertuccelli, O. Toupet, L. Brunet, A. Bachrach, and N. Roy, "Increasing autonomy of UAVs," *IEEE Robotics and Automation Magazine*, vol. 16, pp. 43–51, 2009.

[24] M. de Berg, M. van Kreveld, M. Overmars, and O. Schwarzkopf, "Computational Geometry: Algorithms and Applications," *Springer-Verlag*, 2000.